RESEARCH ARTICLE



Evaluation of Aquifer Properties to Categorize Groundwater Potential in a Part of Southwest Bangladesh Using Catastrophe Theory

Md. Nasir Uddin Khan* and Md. Nozibul Haque

ABSTRACT

This paper evaluated aquifer properties in a part of Southwest Bangladesh to categorize groundwater potential using catastrophe theory (CT). Satellite image, lithologic, pumping test, rainfall and groundwater monitoring data were utilized for this purpose. Lithology-based stratigraphic crosssections confirm six vertically distributed layers, classified into aquitard composed of surface clay with silt and very fine-grained sand with thickness varying from 1 to -24.4 m, whereas the aquifer comprising fine to coarse sand with 3-67 m thick. Pre- and post-monsoon average annual groundwater levels fluctuate from in 3.12 to 3.86 m and 6.97 to 8.36 m, respectively, while average annual recharge ranges from 0.4 to 0.59 m/yr. Groundwater potential index (GWPI) values, validated with specific capacity records, classified the study area into three zones with GWPI of 0.72-0.81 (moderately good), 0.81-0.87 (good), and 0.87-0.96 (very good), covering 25.44%, 47.60%, and 26.96% of the area, respectively. Sensitivity analysis identified rainfall as the most influential and land type as the least influential factor in defining groundwater potentiality. These results can serve as a foundation for the formulation of guidelines and recommendations for the governmental and affiliated agencies for future groundwater exploration, planning, and management.

Keywords: Aquifer property, Groundwater potential zone. Hydrostratigraphy, Sensitivity analysis.

Submitted: October 27, 2023 Published: December 22, 2023

🚭 10.24018lejgeo.2023.4.6.435

Department of Electrical and Electronic Engineering. Islamic University. Bangladesh.

*Corresponding Author: e-mail: mnukhaneee@gmail.com

1. Introduction

Water insufficiency is a major global concern due to its direct influence on people's living standards and economic development [1]. Presently, it provides about 50% of total drinking water [2] and nearly 43% of total irrigation needs globally [3].

Approximately 97% of the Bangladeshi population uses under-groundwater for drinking while 70% of irrigation activities being sustained by groundwater sources [4]. The gross domestic product (GDP) of Bangladesh is heavily reliant on the development of water resources as a whole. Agriculture contributes approximately 30% to the GDP and employs about 60% of labor manpower [5]. The government's agricultural strategy in Bangladesh, as outlined in documents such as MPO [6] in 1991 and WARPO [7] in 2001, places significant emphasis on the development of groundwater resources for purposes that include irrigation and others.

The particular geographical area under consideration is situated in the lower Ganges basin in southwest Bangladesh. This region is predominantly rural and lacks significant industrialization. Its economic dependence is primarily centered on agriculture, characterizing the agro-economic as well as socio-economic factors. The advancement and well-being of this area are closely tied to the effective utilization of its land, particularly through dependable irrigation.

In recent years, the Ganges River has experienced reduced freshwater availability in dry months. This limitation has constrained the potential for surface water resource development, leading the local population to increasingly turn to agriculture dependent on groundwater [8], [9].

The overall hydrogeological conditions of the present study area and its adjacent zones, along with related research, have been thoroughly reviewed by examining various literature sources [6], [9]-[12]. The intensity of irrigation is notably high at 52.95%, and the area under groundwater-based irrigation has been steadily increasing. However, the area also faces natural hazards that impact agricultural production, primarily droughts and occasional floods.

By employing a weighted model that considers logical criteria. GIS can generate thematic maps that contribute to the assessment of groundwater potential [13]–[15]. However, using a Catastrophe theory-based approach mitigates potential bias in weight assignment. This method relies on an internal procedure to ascertain the relative importance of each criterion, thereby diminishing subjectivity, as explained by Yang et al. [16] in 2012.

The key goals of this investigation are to evaluate aquifer properties to categorize groundwater potentials within the area studied employing catastrophe theory in the GIS framework.

1.1. Site Information

The current research area encompasses the Bheramara Upazila (Sub-district) within the Kushtia district (longitude: 88°54′47′–89°03′29″ E and latitude 23°59′13″– 24°07′52″ N), covering a total area of 150.49 km², as depicted in Fig. 1. The primary surface water sources within this region include the Ganges and the Hisna, a distributary of the Ganges. The majority of the area is characterized by low-lying floodplains that have been shaped by alluvial soil deposition.

2. Materials and Methods

The satellite image, borehole lithology, pumping test and groundwater monitoring data were utilized in this study. Following is a breakdown of the data and their sources:

- i) SRTM DEM data $(30 \text{ m} \times 30 \text{ m})$ from USGS,
- ii) Geological map from Geological Survey Bangladesh (GSB),
- iii) Lithologic, pumping test and groundwater monitoring data from Bangladesh Agricultural Development Corporation (BADC), Kushtia.
- iv) Rainfall data from Bangladesh Meteorological Department.
- v) Landsat-7 image from CEGIS, Dhaka.

These data were processed, analyzed and interpreted using Rockworks/2002, SURFER 8.0 and ArcGIS10.4.2 for the quantitative evaluation of the groundwater system spatially and vertically. Entire methodology of this study is shown in Fig. 2.

2.1. Surface Features from Remote Sensing Data

The GIS is used for mapping different features from remote sensing and other data using inverse distance weighted (IDW) interpolating method.

2.1.1. *Land Type*

Landforms exert a direct effect on the presence and flow of groundwater. To categorize the types of landforms for this study, a map was generated using SRTM DEM data within the ArcGIS environment.

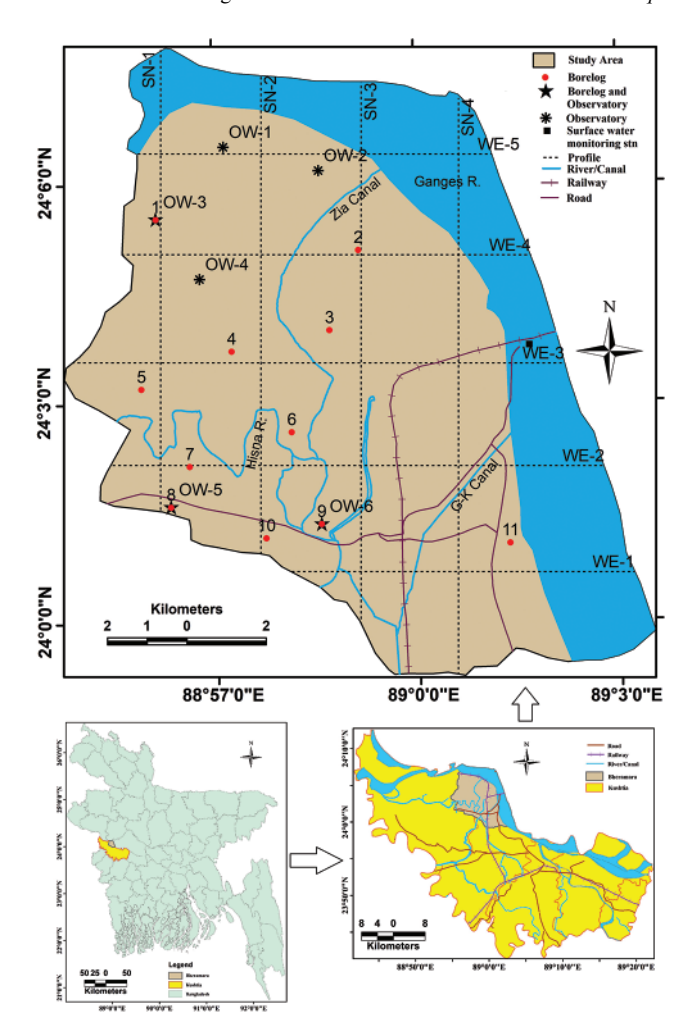


Fig. 1. Key map of the study area.

2.1.2. Slope

The slope of a terrain is a crucial factor influencing the percolation of groundwater into the underground formation. It can be calculated in degrees as the inverse tangent of the rise-to-run ratio.

2.1.3. Drainage Density

It is the length of drainage channel with in a given area. The methodology involved conceptualizing circles around each raster cell center using a specified search radius in ArcGIS. The drainage length falling within these circles was then multiplied by its associated population field value. These values were aggregated, and the total was divided by the circle's area to determine drainage density.

2.1.4. Surface Water Bodies (SWB)

The groundwater storage is replenished by the natural surface sources and have a substantial impact on the groundwater potential in their vicinity [17], [18].

NDVI is one of the easiest ways to find surface water bodies of an area. It is defined as:

$$NDVI = (N_{ir} - V_r)/(N_{ir} + V_r)$$
 (1)

where N_{ir} and V_r represent near infrared and visible (red) band respectively. Water bodies produce negative NDVI values because for water, the red reflectance (V_r) is greater

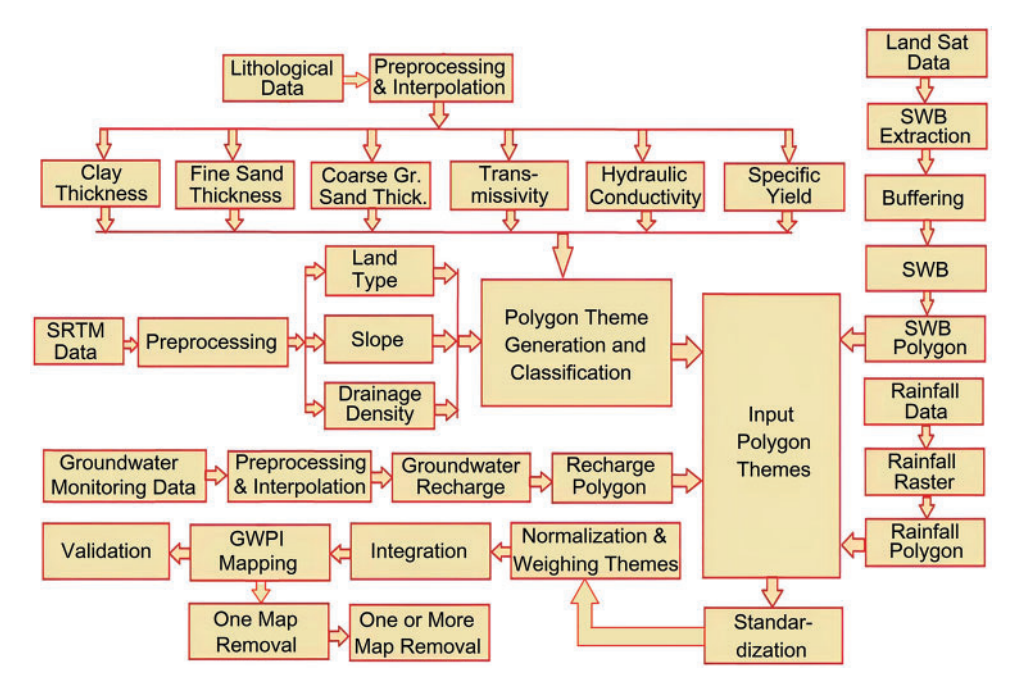


Fig. 2. Flow diagram.

than the near-infrared reflectance (N_{ir}) , as explained by Shopan et al. [19] in 2013.

2.2. Hydrostratigraphy

The occurrence, mobility, quality, and availability of groundwater are governed by subsurface geologic formations' type, distribution, and structure. Stratigraphy is the study of how distinct beds are related to one another and how they form throughout different periods of time. Hydrostratigraphy is a subset of stratigraphy that focuses on groundwater-bearing formations. It is possible to divide hydrostratigraphic units into aquifers and aquitards. Based on eleven lithological records, the present study examined the subsurface geology of the area down to 91 m depth. In order to create the area's 3D model and fence diagrams, Rockworks/2002 was used.

2.3. Rainfall and Recharge

Rainfall, a primary and most substantial contributor to groundwater, plays a vital role in hydrologic cycle. Assessment of rainfall in this region was conducted by analyzing data gathered from 35 weather stations located across Bangladesh as no rainfall station situated inside the area of interest. Over a span of 23 years (2000–2022), the average annual rainfall data from these stations were interpolated for preparing a spatial map depicting the distribution of rainfall in the area.

In this analysis, groundwater table rise from the end of pre-monsoon to the end of monsoon was utilized to estimate recharge. An area's groundwater storage (S_{gw}) may be determined with the use of the following formula:

$$S_{gw} = \Delta h \times S_{v} \tag{2}$$

where rising height is denoted by Δh , and specific yield per unit input formation by S_v . Data on groundwater levels collected from nine sites between 2012 and 2020 were used to calculate site-specific groundwater recharge using (2).

2.4. Aquifer Properties

The aquifer's storage coefficient and transmissivity, respectively, describe the expansion to which groundwater may be accumulated and transmitted via the cracks in the underlying geological structure. These properties can be estimated by analyzing data from single-well aquifer tests. However, in this study, the aquifer parameters were estimated using standard values of aquifer hydraulic conductivity and specific yield.

2.4.1. Transmissivity

Understanding an aquifer's potential to transfer groundwater is crucial for assessing its water supply capacity. Estimating aquifer transmissivity allows for a more thorough evaluation of the hydrogeological properties of the aquifer [20]. The aquifer's transmissivity (T) can be estimated utilizing (3):

$$T = \sum (K_i b_i) \tag{3}$$

where b_i and K_i represent i^{th} layer's unit thickness and hydraulic conductivity, respectively. In this study, the hydraulic conductivity for different formations was adopted from Morris and Johnson [21], as shown in Table I.

TABLE I: THE TYPICAL VALUES OF HYDRAULIC CONDUCTIVITY AND SPECIFIC YIELD OF LITHOLOGIES FOUND IN THE STUDY AREA [21]

		. ,
Materials	Hydraulic cond. (m/day)	Sp. yield (%)
Clay	0.0002	3
Silt	0.08	23
Fine sand	2.5	25.5
Fine-medium sand	7.25	28
Medium sand	12	27.5
Medium to coarse sand	28.5	27
Coarse sand-gravels	45	25.5

2.4.2. Hydraulic Conductivity

Hydraulic conductivity is essential for determining the efficiency with which fluid moves into soil matrix having unit hydraulic head gradient over a specific period. It can be determined by the following (4):

$$K = T/b \tag{4}$$

2.4.3. Specific Yield

The specific yield of a geological formation can be determined by several methods [22]–[24]. In this investigation, the specific yield estimation approach presented by Johnson [22] in 1967, as illustrated in Table I, is applied. It is possible to calculate a figure for the average specific yield by weighting:

$$S_{y} = \frac{(M_{1}m_{1} + M_{2}m_{2} + \ldots + M_{n}m_{n})}{(M_{1} + M_{2} + \ldots + M_{n})}$$
 (5)

where m and M are specific yield and unit thickness for the corresponding formation in percentage.

2.5. IDW Interpolation

In the creation of the maps, the IDW interpolation method was employed. The equation used for IDW interpolation is:

$$H_p = \left(\sum_{i=1}^n \frac{h_i}{d_i^2}\right) / \left(\sum_{i=1}^n \frac{1}{d_i^2}\right)$$
 (6)

In this context for point P, H_p represents the interpolated value, h_i denotes the data point utilized, d_i is the distances between these points, and n signifies the overall count of the points taken into account.

2.6. Groundwater Potential Index (GWPI)

GWPI is a numerical value that can be employed to assess and rank the probability of groundwater occurrences. Using ArcGIS10.4.2, it is possible to transform the different thematic maps into polygon themes. The union tool in ArcGIS was utilized to combine the thematic layers' weights linearly, using the following (7):

$$GWPI = \sum (R_i \times W_i) / \sum W_i \tag{7}$$

where R_i and W_i represent the rating and weight of the i^{th} layer. The integration analysis's most important steps are determining the feature ratings and layer weights, as they impact the final product the most. Each thematic layer was evaluated and given a relative importance score using the catastrophe multi-criteria decision analysis (MCDA).

2.7. Catastrophe Theory (CT)

The decision maker's judgement can be removed from the MCDA technique using catastrophe theory. Instead, its internal process determines which criteria are more important than others, drastically reducing subjectivity [16]. The discontinuity transform was designed to analyze and understand non-linear behavior in dynamic systems [25]. A non-linear and discontinuous change in a system is suitable for this theory [26]. Dependent state variables and control variables are identified in CT as determinants of system performance. Whereas the state variables represent the system's internal token variables, the control variables represent external elements that affect the system [27]. To address complex problems, it is necessary to break the dynamic system into smaller sub-systems, each of which will have its own assessment indications. Subsequently, catastrophe models and fuzzy mathematics are applied to resolve the incongruence in the initial data by standardizing it within the 0-1 range [28]. In Table II, x stands for the state variable, while a, b, c, and d stand for the control variables of seven catastrophe models [29]. The three primary phases of CT implementation are as follows:

2.7.1. Indicator Selection

To evaluate groundwater potential, the groundwater system as a whole is considered as a system, while all the themes were treated as sub-systems.

2.7.2. Standardization

As different thematic layers have different measurement units, raw data values need to be converted to dimensionless quantities ranging from 0 to 1. Li et al. [30] introduced standardization formulas using the 'larger the better' and 'smaller the better' concepts:

$$x_i' = \left[x_i - x_{i(min)}\right] / \left[x_{i(max)} - x_{i(min)}\right]$$
(8)

$$x'_{i} = [x_{i(max)} - x_{i}] / [x_{i(max)} - x_{i(min)}]$$
 (9)

where i, x_i , $x_{i(max)}$ and $x_{i(min)}$ are the index, the original value of i, maximum and minimum values, respectively.

TABLE II: CATASTROPHE MODELS AND NORMALIZATION FORMULAS FOR CT [36]

Catastrophe model	Control parameter	State variable	Potential function	Normalization formula	
Fold	1	1	$V_a(x) = 0.333x^3 + ax$	$x_a = a^{1/2}$	
Cusp	2	1	$V_{ab}(x) = 0.25x^4 + 0.5ax^2 + bx$	$x_a = a^{1/2}, x_b = b^{1/3}$	
Swallowtail	3	1	$V_{abc}(x) = 0.2x^5 + 0.333ax^3 + 0.5bx^2 + cx$	$x_a = a^{1/2}, x_b = b^{1/3}$ and $x_c = c^{1/4}$	
Butterfly	4	1	$V_{abcd}(x) = 0.17x^6 + 0.25ax^4 + 0.33bx^3 + 0.5cx^2 + dx$	$x_a = a^{1/2}, x_b = b^{1/3}, x_c = c^{1/4} \text{ and } x_d = d^{1/5}$	
Oval umb. Point	3	2	$V_{abc}(x, y) = x^3 + y^3 + axy + bx + cy$		
Elliptic umb. Point	3	2	$V_{abc}(x, y) = x^3 - xy^2 + a(x^2 + y^2) + bx + cy$		
Parabolic umb. Point	4	2	$V_{abcd}(x, y) = x^2y + x^4 + ax^2 + by^2 + cx + dy$		

2.7.3. Normalization

Standardization is performed using the appropriate normalizing formulas of Table II, which vary depending on the catastrophe model being fitted to the input data.

Complementary and non-complementary methods are widely employed for recursive computations in the normalization process [31]. The complementary rule states that the sub-system's a, b, c, and d control variables cancel each other out. Therefore, they all gravitate toward the mean value $x = (x_a + x_b + x_c + x_d)/4$ [32]. The state variable's value in the noncomplementary rule is determined by selecting the smallest of the subsystem's control variables $(x = min \{x_a, x_b, x_c, x_d\})$ [33]. Since the study's control variables are mutually reinforcing, the complementary rule was used to calculate the control variables' respective catastrophe progressions.

2.8. Sensitivity Analysis

The sensitivity analysis results may be used to estimate how much weight to give to various factors. As a rule, map-removal and single-parameter methods are utilized to conduct this investigation. One or more maps were eliminated to determine the effect of input parameters on the output [34], [35], and this approach was used to evaluate the consistency of the analytical results:

$$S = 100 \times (V - V')/V \tag{10}$$

where V denotes unperturbed whereas V' represents perturbed indices.

2.9. Groundwater Potential Zone Validation

Groundwater potential zones of the study area were validated using specific capacity (S_c) data estimated from single-well pumping test results. The specific capacity of a formation is determined as the drawdown (S_w) per unit discharge $(Q_{\rm w})$:

$$S_c = S_w / Q_w \tag{11}$$

3. RESULTS AND DISCUSSIONS

3.1. Thematic Layers

3.1.1. Land Type (LT)

Based on elevation relative to mean sea level (MSL), the area was categorized into four classes: very lowland (-2-6 m), lowland (6–13 m), medium highland (13–19 m), and highland (19–23 m), as illustrated in Fig. 3(a). It's worth noting that higher elevated land tends to result in increased runoff and reduced infiltration capacity. Therefore, in the rating scheme (Table III), a lower rating is assigned to the highland areas.

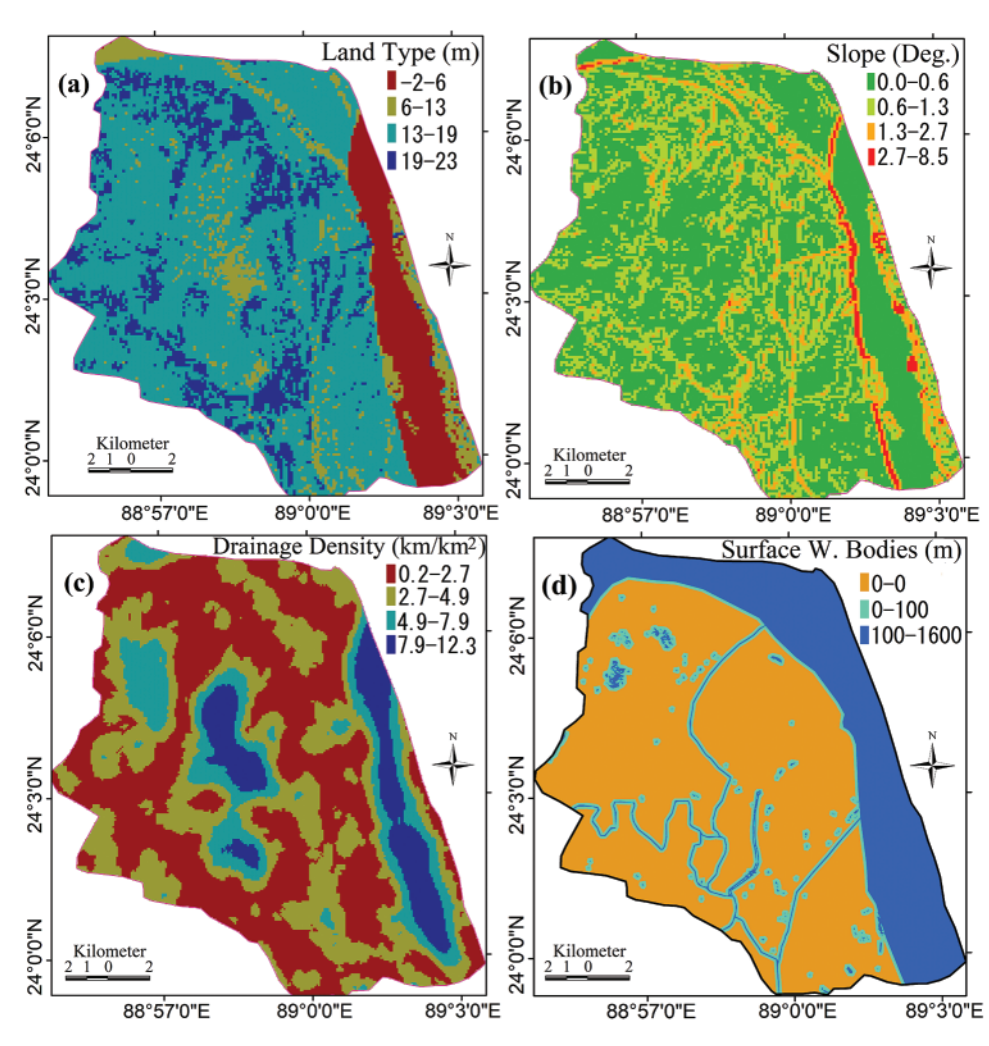


Fig. 3. Spatial variation of (a) Land types, (b) slope, (c) DD, and (d) SWB.

TABLE III: RATINGS AND WEIGHTS OF VARIOUS THEMATIC MAPS AND THEIR FEATURES

(B1) Medium highland (C2) 13–19 16.0 0.12 0.50 Lowland (C3) 6–13 9.5 0.21 0.68 Very lowland (C4) -2–6 4.0 1.00 1.00 Slope in degree Very steep (C5) 2.7–8.5 5.6 0.06 0.24 0.63 0.0635 (B2) Medium steep (C6) 1.3–2.7 2.0 0.16 0.54 Low steep (C7) 0.6–1.3 0.95 0.33 0.76 Very low steep (C8) 0.0–0.6 0.3 1.00 1.00 Drainage Very high-dense system 7.9–12.3 10.1 0.14 0.38 0.69 0.0697 density in (C9) km.km² (B3) High dense system (C10) 4.9–7.9 6.4 0.23 0.61 Medium dense system (C11) 4.9–7.9 3.80 0.38 0.79 (C11) Low dense system (C12) 0.2–2.7 1.45 1.00 1.00 Surface water Less favorable (C13) 100–1600 850 0 0 0.00 0.66 0.0663	Sub-system	Indicators	Range of index value	Avg. index value	Standardized value	Normalized rating value	Av. normalized rating value	Weight
Court Cour	Land type in m	Highland(C1)	19–23	21.0	0.10	0.31	0.62	0.0624
Neg Normal (C4) 1.00 1.0	(B1)	Medium highland (C2)	13–19	16.0	0.12	0.50		
Slope in degree Very steep (C5) 2.7-8.5 5.6 0.06 0.24 0.63 0.0635 Medium steep (C7) 0.6-1.3 0.95 0.33 0.76 Very low steep (C8) 0.0-0.6 0.3 1.00 1.00 Drainage density in Very high-classe system C(9) 0.9-1.3 0.10 0.14 0.38 0.69 0.0697 Emissity in Very high-classe system C(9) 0.2-2.7 1.45 1.00 1.00 0.06 Surface water Cestavorable (C13) 0.2-2.7 1.45 1.00 1.00 0.06 0.0663 Ordinary of the province		Lowland (C3)	6–13	9.5	0.21	0.68		
Medium steep (C6)		Very lowland (C4)	-2-6	4.0	1.00	1.00		
Low steep (C7) 0.6-1.3 0.95 0.33 0.76	Slope in degree	Very steep (C5)	2.7-8.5	5.6	0.06	0.24	0.63	0.0635
New Notion	(B2)	Medium steep (C6)	1.3-2.7	2.0	0.16	0.54		
Drainage density in (C9)		Low steep (C7)	0.6-1.3	0.95	0.33	0.76		
Memistry in CO Minshift CO Minshift Migh dense system (CI) Color CI) C		Very low steep (C8)	0.0 – 0.6	0.3	1.00	1.00		
km.km² (B3) High dense system (C10) 4.9-7.9 6.4 0.23 0.61 well (C11) 2.7-4.9 3.80 0.38 0.79 Surface water code water solding in m (B4) Less favorable (C12) 0.2-2.7 1.45 1.00 1.00 Surface water solding in m (B4) Favorable (C13) 0.0-1600 850 0.94 0.98 High (C16) 17.3-24.4 20.85 0.25 0.50 0.70 0.75 0.075 Clay thickness in m (B4) High (C16) 13.3-17.3 11.3 0.46 0.82 in m (B5) Moderately high (C17) 13.3-17.3 11.3 0.46 0.82 Low (C19) 1.0-9.3 5.15 1.00 1.00 Fine sand Low (C20) 3.0-11.2 7.1 0.31 0.56 0.83 0.083 thish (C23) 18.3-27.4 22.85 1.00 1.00 1.00 1.00 1.00 1.00 1.00 1.00 1.00 1.00 1.00 1.00 1.00 1.00 1.00	Drainage	Very high-dense system	7.9-12.3	10.1	0.14	0.38	0.69	0.0697
Medium dense system (C12) 0.2-2.7 1.45 1.00 1.00 1.00	density in	(C9)						
Medium dense system (C12) 0.2-2.7 1.45 1.00 1.00 1.00	km.km ² (B3)	High dense system (C10)	4.9-7.9	6.4	0.23	0.61		
Surface water books in (B4) protection in (B4)		Medium dense system	2.7–4.9	3.80	0.38	0.79		
colicies in m (B4) Favorable (C14) 0-100 50 0.94 0.98 Clay thickness High (C16) 17.3-24.4 20.85 0.25 0.50 0.75 0.0758 in m (B5) Moderately high (C17) 13.3-17.3 15.3 0.34 0.70 0.075 0.0758 Fine sand Low (C19) 1.0-9.3 5.15 1.00 1.00 0.83 0.833 0.833 thickness Medium (C21) 11.2-15.0 13.1 0.57 0.83 0.083 in m (B6) Moderately high (C22) 15.0-18.3 16.65 0.73 0.92 0.94 0.0949 sand thickness Medium (C23) 18.3-27.4 22.85 1.00 1.00 0.00 0.00 0.04 0.0949 0.0949 0.0949 0.0949 0.0949 0.0949 0.0949 0.094 0.0949 0.0949 0.0949 0.094 0.0949 0.0949 0.094 0.0949 0.0949 0.0949 0.0949 0.0949 0.0949 0.0949 0.0949 </td <td></td> <td>Low dense system (C12)</td> <td>0.2 - 2.7</td> <td>1.45</td> <td>1.00</td> <td>1.00</td> <td></td> <td></td>		Low dense system (C12)	0.2 - 2.7	1.45	1.00	1.00		
Highly favorable (C15) 0-0 0 1 1.00	Surface water		100-1600	850	0	0.00	0.66	0.0663
Clay thickness in m (B5) High (C16) 17.3-24.4 20.85 0.25 0.50 0.75 0.0758 in m (B5) Moderately high (C17) 13.3-17.3 15.3 0.34 0.70 0.0758 Medium (C18) 9.3-13.3 11.3 0.46 0.82 0.00 0.00 Fine sand Low (C20) 3.0-11.2 7.1 0.31 0.56 0.83 0.0833 thickness Medium (C21) 11.2-15.0 13.1 0.57 0.83 0.92 in m (B6) Moderately high (C22) 15.0-18.3 16.65 0.73 0.92 High (C23) 18.3-27.4 22.85 1.00 1.00 0.00 Coarse grained Sand thickness Medium (C25) 50.3-53.3 51.80 0.83 0.94 0.0949 sand thickness Medium (C25) 50.3-53.3 51.80 0.89 0.97 0.097 1.00 1.00 1.00 1.00 1.00 1.00 1.00 1.00 1.00 1.00 1.00 1.00 1.00 1.00 1.00 1.00	bodies in m (B4)	Favorable (C14)	0-100	50	0.94	0.98		
Clay thickness in High (C16)	· ´	Highly favorable (C15)	0–0		1	1.00		
in m (B5) Moderately high (C17) 13.3-17.3 15.3 0.34 0.70 Medium (C18) 9.3-13.3 11.3 0.46 0.82 Low (C19) 1.0-9.3 5.15 1.00 1.00 Fine sand thickness Low (C20) 3.0-11.2 7.1 0.31 0.56 0.83 0.0833 thickness Medium (C21) 11.2-15.0 13.1 0.57 0.83 0.0833 in m (B6) Moderately high (C22) 15.0-18.3 16.65 0.73 0.92 High (C23) 18.3-27.4 22.28.5 1.00 1.00 Coarse grained Low (C24) 42.7-50.3 46.50 0.75 0.86 0.94 0.0949 sand thickness Medium (C25) 53.3-57.6 55.45 0.89 0.97 0.97 High (C27) 57.6-67.0 62.30 1.00 1.00 1.00 1.00 Transmissivity Medium (C28) 2114-2256 2185 0.87 0.93 0.97 0.097 High (C30) </td <td>Clay thickness</td> <td>• • • • • • • • • • • • • • • • • • • •</td> <td>17.3-24.4</td> <td>20.85</td> <td>0.25</td> <td></td> <td>0.75</td> <td>0.0758</td>	Clay thickness	• • • • • • • • • • • • • • • • • • • •	17.3-24.4	20.85	0.25		0.75	0.0758
Medium (C18)	•							
Fine sand Low (C19) 1.0–9.3 5.15 1.00 1.00 Fine sand Low (C20) 3.0–11.2 7.1 0.31 0.56 0.83 0.833 thickness Medium (C21) 11.2–15.0 13.1 0.57 0.83 in m (B6) Moderately high (C22) 15.0–18.3 16.65 0.73 0.92 High (C23) 18.3–27.4 22.85 1.00 1.00 Coarse grained Low (C24) 42.7–50.3 46.50 0.75 0.86 0.94 0.949 sand thickness Medium (C25) 50.3–53.3 51.80 0.83 0.94 in m (B7) Moderately high (C26) 53.3–57.6 55.45 0.89 0.97 High (C27) 57.6–67.0 62.30 1.00 1.00 Transmissivity Medium (C28) 2114–2256 2185 0.87 0.93 0.97 High (C30) 2347–2452 2399.5 0.95 0.99 Very high (C31) 2452–2591 2521.5 1.00 1.00 Hydraulic Medium (C32) 28.2–32.4 30.3 0.73 0.86 0.94 Moderately high (C30) 32.4–35.2 33.8 0.82 0.94 "Moderately high (C33) 32.4–35.2 33.8 0.82 0.94 "Moderately high (C34) 35.2–38.3 36.75 0.89 0.97 Very high (C35) 38.3–44.2 41.25 1.00 1.00 Specific yield in Medium (C36) 18.9–21.1 20.0 0.81 0.90 Wery high (C39) 23.5–26.0 24.75 0.88 0.96 "Wery high (C39) 23.5–26.0 24.75 0.88 0.96 Very high (C39) 23.5–26.0 24.75 0.88 0.96 Very high (C39) 23.5–26.0 24.75 0.88 0.96 Wery high (C39) 23.5–26.0 24.75 0.88 0.96 Wery high (C39) 23.5–26.0 24.75 0.93 0.98 Very high (C39) 23.5–26.0 24.75 0.98 0.998 Wery high (C39) 1462–1465 1463.50 0.9949 0.998 Moderately high (C42) 1465–1467 1465.98 0.9965 0.9988 Moderately high (C42) 1466–1467 1465.98 0.9965 0.9988 Moderately high (C42) 1467–1469 1468.00 0.9980 0.9995 High (C43) 1469–1473 1471.00 1.0000 1.0000 Recharge in Medium (C44) 0.40–0.45 0.425 0.76 0.87 0.95 0.0950 Myr (B12) Moderately high (C44) 0.40–0.45 0.425 0.76 0.87 0.95 0.0950 Myr (B12) Moderately high (C45) 0.45–0.47 0.460 0.83 0.99 Myr (B12) Moderately high (C44) 0.40–0.45 0.425 0.76 0.87 0.95 0.0950 Myr (B12) Moderately high (C44) 0.40–0.45 0.425 0.76 0.89 0.99		• • •						
Fine sand thickness Low (C20) 3.0–11.2 7.1 0.31 0.56 0.83 0.0833 thickness in m (B6) Medium (C21) 11.2–15.0 13.1 0.57 0.83 in m (B6) Moderately high (C22) 15.0–18.3 16.65 0.73 0.92 High (C23) 18.3–27.4 22.85 1.00 1.00 Coarse grained sand thickness Medium (C24) 42.7–50.3 46.50 0.75 0.86 0.94 0.0949 sand thickness Medium (C25) 50.3–53.3 51.80 0.83 0.94 0.0949 sand thickness Medium (C25) 50.3–53.3 51.80 0.83 0.94 0.0949 sand thickness Medium (C25) 50.3–53.3 51.80 0.83 0.94 0.094 in m (B7) Medium (C25) 50.3–53.3 51.80 0.89 0.97 Transmissivity Medium (C26) 214–2256 2185 0.87 0.93 0.97 0.097 Transmissivity Medium (C30) 2452–2591		` ′						
thickness in m (B6)	Fine sand						0.83	0.0833
in m (B6) Moderately high (C22) 15.0-18.3 16.65 0.73 0.92 Coarse grained Low (C24) 18.3-27.4 22.85 1.00 1.00 Coarse grained Low (C24) 42.7-50.3 46.50 0.75 0.86 0.94 0.0949 sand thickness Medium (C25) 50.3-53.3 51.80 0.83 0.94 0.97 in m (B7) Moderately high (C26) 53.3-57.6 55.45 0.89 0.97 High (C27) 57.6-67.0 62.30 1.00 1.00 Transmissivity Medium (C28) 2114-2256 2185 0.87 0.93 0.97 0.0977 High (C30) 2347-2452 2399.5 0.95 0.99 0.99 0.97 0.97 0.97 0.97 0.97 0.97 0.91 0.90 0.99 0.99 0.99 0.99 0.99 0.99 0.99 0.99 0.99 0.99 0.99 0.99 0.99 0.99 0.99 0.99 0.99 0.99							0.02	0.0022
Coarse grained Low (C24) 42.7-50.3 46.50 0.75 0.86 0.94 0.0949		` ′						
Coarse grained sand thickness Low (C24) 42.7–50.3 46.50 0.75 0.86 0.94 0.0949 sand thickness in m (B7) Moderately high (C26) 50.3–53.3 51.80 0.83 0.94 in m (B7) Moderately high (C26) 53.3–57.6 55.45 0.89 0.97 High (C27) 57.6–67.0 62.30 1.00 1.00 Transmissivity Medium (C28) 2114–2256 2185 0.87 0.93 0.97 0.0977 in m²/day (B8) Moderately high (C29) 2256–2347 2301.5 0.91 0.97 0.97 0.0977 Hydraulic Medium (C30) 2347–2452 2399.5 0.95 0.99	m m (B0)							
sand thickness in m (B7) Moderately high (C26) 53.3–57.6 55.45 0.89 0.97 High (C27) 57.6–67.0 62.30 1.00 1.00 1.00 1.00 1.00 1.00 1.00 1	Coarse grained						0.94	0 0949
in m (B7) Moderately high (C26) 53.3-57.6 55.45 0.89 0.97 High (C27) 57.6-67.0 62.30 1.00 1.00 Transmissivity Medium (C28) 2114-2256 2185 0.87 0.93 0.97 0.0977 in m²/day (B8) Moderately high (C29) 2256-2347 2301.5 0.91 0.97 0.97 High (C30) 2347-2452 2399.5 0.95 0.99 0.99 0.97 0.97 0.97 0.97 0.97 0.96 0.94							0.51	0.05 15
High (C27) 57.6-67.0 62.30 1.00 1.00 Transmissivity Medium (C28) 2114-2256 2185 0.87 0.93 0.97 0.0977 in m²/day (B8) Moderately high (C29) 2256-2347 2301.5 0.91 0.97 High (C30) 2347-2452 2399.5 0.95 0.99 Very high (C31) 2452-2591 2521.5 1.00 1.00 Hydraulic Medium (C32) 28.2-32.4 30.3 0.73 0.86 0.94 0.0946 conductivity in Moderately high (C33) 32.4-35.2 33.8 0.82 0.94 m/day (B9) High (C34) 35.2-38.3 36.75 0.89 0.97 Very high (C35) 38.3-44.2 41.25 1.00 1.00 Specific yield in Medium (C36) 18.9-21.1 20.0 0.81 0.90 0.96 0.0964 % (B10) Moderately high (C37) 21.1-22.4 21.75 0.88 0.96 High (C38) 22.4-23.5 22.95 0.93 0.98 Very high (C39) 23.5-26.0 24.75 1.00 1.00 Rainfall in mm Low (C40) 1462-1465 1463.50 0.9949 0.9974 0.9989 0.1004 (B11) Medium (C41) 1465-1467 1465.98 0.9965 0.9988 Moderately high (C42) 1467-1469 1468.00 0.9980 0.9995 High (C43) 1469-1473 1471.00 1.0000 Recharge in Medium (C44) 0.40-0.45 0.425 0.76 0.87 0.95 0.0950 m/yr (B12) Moderately high (C45) 0.45-0.47 0.460 0.83 0.94 High (C46) 0.47-0.52 0.495 0.89 0.97								
Transmissivity Medium (C28) 2114-2256 2185 0.87 0.93 0.97 0.0977 in m²/day (B8) Moderately high (C29) 2256-2347 2301.5 0.91 0.97 High (C30) 2347-2452 2399.5 0.95 0.99 Very high (C31) 2452-2591 2521.5 1.00 1.00 Hydraulic Medium (C32) 28.2-32.4 30.3 0.73 0.86 0.94 0.0946 conductivity in Moderately high (C33) 32.4-35.2 33.8 0.82 0.94 m/day (B9) High (C34) 35.2-38.3 36.75 0.89 0.97 Very high (C35) 38.3-44.2 41.25 1.00 1.00 Specific yield in Medium (C36) 18.9-21.1 20.0 0.81 0.90 0.96 % (B10) Moderately high (C37) 21.1-22.4 21.75 0.88 0.96 High (C38) 22.4-23.5 22.95 0.93 0.98 Very high (C39) 23.5-26.0 24.75 1.00 1.00 Rainfall in mm Low (C40) 1462-1465 1463.50 0.9949 0.9974 0.9989 0.1004 (B11) Medium (C41) 1465-1467 1465.98 0.9965 0.9988 Moderately high (C42) 1467-1469 1468.00 0.9980 0.9995 High (C43) 1469-1473 1471.00 1.0000 1.0000 Recharge in Medium (C44) 0.40-0.45 0.425 0.76 0.87 0.95 0.0950 m/yr (B12) Moderately high (C45) 0.45-0.47 0.460 0.83 0.94 High (C46) 0.47-0.52 0.495 0.89 0.97	m m (B7)							
in m²/day (B8)	Transmissivity						0.97	0.0977
High (C30) 2347–2452 2399.5 0.95 0.99 Very high (C31) 2452–2591 2521.5 1.00 1.00 Hydraulic Medium (C32) 28.2–32.4 30.3 0.73 0.86 0.94 0.0946 conductivity in Moderately high (C33) 32.4–35.2 33.8 0.82 0.94 m/day (B9) High (C34) 35.2–38.3 36.75 0.89 0.97 Very high (C35) 38.3–44.2 41.25 1.00 1.00 Specific yield in Medium (C36) 18.9–21.1 20.0 0.81 0.90 0.96 0.0964 % (B10) Moderately high (C37) 21.1–22.4 21.75 0.88 0.96 High (C38) 22.4–23.5 22.95 0.93 0.98 Very high (C39) 23.5–26.0 24.75 1.00 1.00 Rainfall in mm (B1) Medium (C41) 1465–1467 1465.98 0.9965 0.9988 Moderately high (C42) 1467–1469 1468.00 0.9980 0.9995 High (C43) 1469–1473 1471.00 1.0000 1.0000 Recharge in Medium (C44) 0.40–0.45 0.425 0.76 0.87 0.95 0.0950 m/yr (B12) Moderately high (C45) 0.45–0.47 0.460 0.83 0.94 High (C46) 0.47–0.52 0.495 0.89 0.97	•	` ′					0.57	0.0777
Very high (C31) 2452-2591 2521.5 1.00 1.00 Hydraulic Medium (C32) 28.2-32.4 30.3 0.73 0.86 0.94 0.0946 conductivity in Moderately high (C33) 32.4-35.2 33.8 0.82 0.94 m/day (B9) High (C34) 35.2-38.3 36.75 0.89 0.97 Very high (C35) 38.3-44.2 41.25 1.00 1.00 Specific yield in Medium (C36) 18.9-21.1 20.0 0.81 0.90 0.96 0.0964 % (B10) Moderately high (C37) 21.1-22.4 21.75 0.88 0.96 High (C38) 22.4-23.5 22.95 0.93 0.98 Very high (C39) 23.5-26.0 24.75 1.00 1.00 Rainfall in mm	m m /day (bo)							
Hydraulic Medium (C32) 28.2–32.4 30.3 0.73 0.86 0.94 0.0946 conductivity in M/day (B9) Moderately high (C33) 32.4–35.2 33.8 0.82 0.94 0.94 m/day (B9) High (C34) 35.2–38.3 36.75 0.89 0.97 Very high (C35) 38.3–44.2 41.25 1.00 1.00 Specific yield in Medium (C36) 18.9–21.1 20.0 0.81 0.90 0.96 0.0964 % (B10) Moderately high (C37) 21.1–22.4 21.75 0.88 0.96 0.96 0.0964 High (C38) 22.4–23.5 22.95 0.93 0.98 0.98 0.98 0.998 0.998 0.998 0.998 0.998 0.998 0.998 0.998 0.998 0.998 0.9989 0.998 0.9989 0.9989 0.9989 0.9989 0.9989 0.9989 0.9989 0.9989 0.9988 0.9988 0.9988 0.9988 0.9988 0.9988 0.9989 0.9989 0.9989								
conductivity in Moderately high (C33) 32.4–35.2 33.8 0.82 0.94 m/day (B9) High (C34) 35.2–38.3 36.75 0.89 0.97 Very high (C35) 38.3–44.2 41.25 1.00 1.00 Specific yield in Medium (C36) 18.9–21.1 20.0 0.81 0.90 0.96 0.0964 % (B10) Moderately high (C37) 21.1–22.4 21.75 0.88 0.96 High (C38) 22.4–23.5 22.95 0.93 0.98 Very high (C39) 23.5–26.0 24.75 1.00 1.00 Rainfall in mm Low (C40) 1462–1465 1463.50 0.9949 0.9974 0.9989 0.1004 (B11) Medium (C41) 1465–1467 1465.98 0.9965 0.9988 Moderately high (C42) 1467–1469 1468.00 0.9980 0.9995 High (C43) 1469–1473 1471.00 1.0000 1.0000 Recharge in Medium (C44) 0.40–0.45 0.425 0.76 0.87 0.95 0.0950 m/yr (B12) Moderately high (C45) 0.45–0.47 0.460 0.83 0.94 High (C46) 0.47–0.52 0.495 0.89 0.97	Hydraulic						0.04	0.0046
m/day (B9) High (C34) 35.2–38.3 36.75 0.89 0.97 Very high (C35) 38.3–44.2 41.25 1.00 1.00 Specific yield in % (B10) Medium (C36) 18.9–21.1 20.0 0.81 0.90 0.96 0.0964 % (B10) Moderately high (C37) 21.1–22.4 21.75 0.88 0.96 0.98 High (C38) 22.4–23.5 22.95 0.93 0.98 0.98 Very high (C39) 23.5–26.0 24.75 1.00 1.00 Rainfall in mm (B11) Low (C40) 1462–1465 1463.50 0.9949 0.9974 0.9989 0.1004 (B11) Medium (C41) 1465–1467 1465.98 0.9965 0.9988 0.9988 0.9995 0.9988 0.9995 0.9988 0.9995 0.9988 0.9995 0.9980 0.9995 0.9995 0.9980 0.9995 0.9995 0.9980 0.9995 0.9980 0.9995 0.9980 0.9995 0.9980 0.9995 0.9980 0.9980 0.9980 0.9980 0.9980 0.9980 0.9980 0.9980 0.9980							0.54	0.0740
Very high (C35) 38.3-44.2 41.25 1.00 1.00	•							
Specific yield in % (B10) Medium (C36) 18.9–21.1 20.0 0.81 0.90 0.96 0.0964 % (B10) Moderately high (C37) 21.1–22.4 21.75 0.88 0.96 High (C38) 22.4–23.5 22.95 0.93 0.98 Very high (C39) 23.5–26.0 24.75 1.00 1.00 Rainfall in mm (B11) Low (C40) 1462–1465 1463.50 0.9949 0.9974 0.9989 0.1004 (B11) Medium (C41) 1465–1467 1465.98 0.9965 0.9988 0.9988 0.9995 0.9988 0.9995 0.9995 0.9995 0.9995 0.9995 0.9995 0.9995 0.9995 0.9995 0.9995 0.9988 0.9965 0.9988 0.9995 0.9988 0.9995 0.9988 0.9995 0.9988 0.9995 0.9988 0.9995 0.9988 0.9995 0.9988 0.9995 0.9988 0.9995 0.9988 0.9965 0.9988 0.9986 0.9995 0.9988 0.9988 0.9965 0.9988<	ili/day (D3)							
% (B10) Moderately high (C37) 21.1–22.4 21.75 0.88 0.96 High (C38) 22.4–23.5 22.95 0.93 0.98 Very high (C39) 23.5–26.0 24.75 1.00 1.00 Rainfall in mm Low (C40) 1462–1465 1463.50 0.9949 0.9974 0.9989 0.1004 (B11) Medium (C41) 1465–1467 1465.98 0.9965 0.9988 Moderately high (C42) 1467–1469 1468.00 0.9980 0.9995 High (C43) 1469–1473 1471.00 1.0000 1.0000 Recharge in Medium (C44) 0.40–0.45 0.425 0.76 0.87 0.95 0.0950 m/yr (B12) Moderately high (C45) 0.45–0.47 0.460 0.83 0.94 High (C46) 0.47–0.52 0.495 0.89 0.97	Specific viold in						0.06	0.0064
High (C38) 22.4–23.5 22.95 0.93 0.98 Very high (C39) 23.5–26.0 24.75 1.00 1.00 Rainfall in mm Low (C40) 1462–1465 1463.50 0.9949 0.9974 0.9989 0.1004 (B11) Medium (C41) 1465–1467 1465.98 0.9965 0.9988 Moderately high (C42) 1467–1469 1468.00 0.9980 0.9995 High (C43) 1469–1473 1471.00 1.0000 1.0000 Recharge in Medium (C44) 0.40–0.45 0.425 0.76 0.87 0.95 0.0950 m/yr (B12) Moderately high (C45) 0.45–0.47 0.460 0.83 0.94 High (C46) 0.47–0.52 0.495 0.89 0.97	-						0.90	0.0904
Very high (C39) 23.5–26.0 24.75 1.00 1.00	70 (B 10)							
Rainfall in mm (B11)								
(B11) Medium (C41) 1465–1467 1465.98 0.9965 0.9988 Moderately high (C42) 1467–1469 1468.00 0.9980 0.9995 High (C43) 1469–1473 1471.00 1.0000 1.0000 Recharge in Medium (C44) 0.40–0.45 0.425 0.76 0.87 0.95 0.0950 m/yr (B12) Moderately high (C45) 0.45–0.47 0.460 0.83 0.94 High (C46) 0.47–0.52 0.495 0.89 0.97	D = i = f = 11 i =	, , ,					0.0000	0.1004
Moderately high (C42) 1467–1469 1468.00 0.9980 0.9995 High (C43) 1469–1473 1471.00 1.0000 1.0000 Recharge in Medium (C44) 0.40–0.45 0.425 0.76 0.87 0.95 0.0950 m/yr (B12) Moderately high (C45) 0.45–0.47 0.460 0.83 0.94 High (C46) 0.47–0.52 0.495 0.89 0.97							0.9989	0.1004
Recharge in Myr (B12) High (C43) 1469–1473 1471.00 1.0000 1.0000 Recharge in Medium (C44) 0.40–0.45 0.425 0.76 0.87 0.95 0.0950 m/yr (B12) Moderately high (C45) 0.45–0.47 0.460 0.83 0.94 High (C46) 0.47–0.52 0.495 0.89 0.97	(B11)							
Recharge in myr (B12) Medium (C44) 0.40-0.45 0.425 0.76 0.87 0.95 0.0950 m/yr (B12) Moderately high (C45) 0.45-0.47 0.460 0.83 0.94 High (C46) 0.47-0.52 0.495 0.89 0.97								
m/yr (B12) Moderately high (C45) 0.45–0.47 0.460 0.83 0.94 High (C46) 0.47–0.52 0.495 0.89 0.97	D. J.						0.05	0.0050
High (C46) 0.47–0.52 0.495 0.89 0.97	-						0.95	0.0950
	m/yr (B12)							
Very high (C47) 0.52–0.59 0.555 1.00 1.00								
		Very high (C47)	0.52-0.59	0.555	1.00	1.00		

3.1.2. Slope (S)

In this study, the slope ranging from 0.0° to 8.5° was classified into four categories: very low steep (0.0°-0.6°), low steep (0.6°-1.3°), medium steep (1.3°-2.7°), and very steep (2.7°–8.5°). Consequently, the areas with the highest slope may be considered to have poor groundwater potential because of lowest surface water infiltration. A visual representation of these features and their corresponding ratings can be found in Fig. 3(b) and Table III, respectively.

3.1.3. Drainage Density (DD)

Based on their relevance to groundwater, the derived DD map was categorized into four classes: lowdense system (0.2-2.7 km/km²), medium-dense system $(2.7-4.9 \text{ km/km}^2)$, high-dense system $(4.9-7.9 \text{ km/km}^2)$, and very high-dense system (7.9–12.3 km/km²). Areas characterized by high drainage density receive a lower rating compared to those with low drainage density (Fig. 3(c) and Table III).

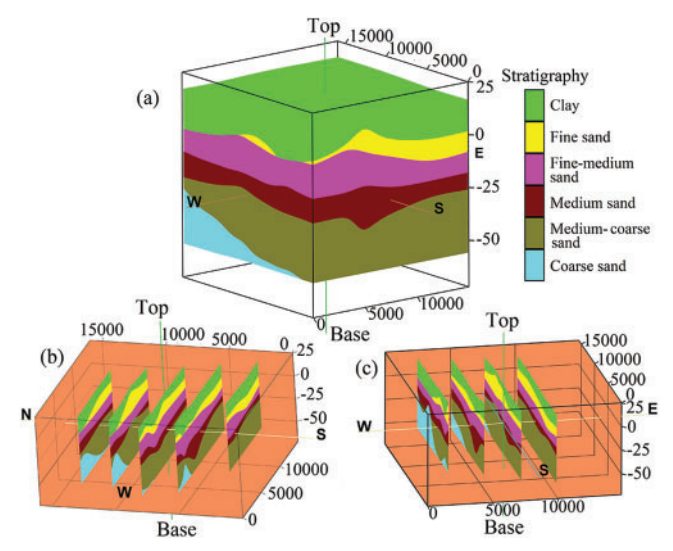


Fig. 4. 3D view of stratigraphic model (a), fence diagrams along the west-east direction (b), and south-north direction (c).

3.1.4. Surface Water Bodies (SWB)

The SWB map was classified into three distinct groups based on their proximity to the nearest water body. Specifically, areas directly adjacent to a water body (0-0 m) were classified as "highly favorable," those within a buffer zone ranging from 0 m to 100 m were considered "favorable," and regions located between 100 m and a maximum of 1600 m from the water body were labeled as "less favorable". This classification is depicted in Fig. 3(d). The corresponding rating are outlined in Table III.

3.1.5. Stratigraphy

The 3-D stratigraphic model prepared using Rockworks/2002 software is shown in Fig. 4(a). To observe the stratigraphic layers with respect to MSL, different illustrative fence diagram along the west-east and south-north profiles was prepared and depicted in Figs. 4(b) and 4(c), respectively. From the figure it reveals that the region predominantly comprises two subsurface strata, specifically an upper clay layer and a sandy formation of varying grain sizes, which potentially serves as a viable aquifer. However, the sandy deposit exhibits distinct subdivisions into fine, fine-medium, medium, medium-coarse, and coarse sands. While the top clay, fine sand, fine-medium sand, and coarse sand layers are consistently present throughout the area, the medium and medium-coarse sands are not uniformly distributed. The cumulative thickness of these multiple water-bearing layers within the region, suitable for productive aquifer use, appears promising. Based on these visual findings, the subsurface geology in the area can be mentioned as favorable for the development of groundwater potential if the other relevant conditions are met.

3.1.5.1. Hydrostratigraphic Units

The development of underground water requires knowledge of the characteristics of sub-surface water-bearing zone, with specific consideration given to its composition and thickness. The groundwater bearing chronological sequence in the area were divided into main two hydrostratigraphic layers: (1) aquitard and (2) aquifer.

Aquitard (Clay)

A relatively slim surface layer, serving as an aquitard, is primarily consisted of clay accompanied by silt and extremely fine sand. Although this geological formation is rather frequent, its thickness varies depending on the local geomorphology. Fig. 5(a) depicts the aguitard thickness geographical map. The majority of the region falls within a depth range of 9.3 to 17.3 m, with areas of 1 to 9.3 m and 17.3 to 24.4 m in thickness scattered throughout the region. This particular layer, due to its notably low permeability and productivity, can only be considered a potential source for dug wells when it comes to groundwater extraction.

Aquifer (Coarse Grained Sands)

A sandy formation with a range of grain sizes acts as the primary aguifer in the area under study. The lithological information in the region has substantiated the existence of aquifer materials with varying granular characteristics, which can be categorized into (1) small scale aquifer and (2) main aquifer.

Small-Scale Aquifer

The lithological data in the region confirm the presence of a layer comprising primarily fine sand with occasional fine-medium sand, located just beneath the upper aquitard layer as shown in Fig. 5(b), the thickness being varying from 3 to 27.4 m. Approximately 85% of the area falls within a thickness range of 11.2 to 18.3 m, while the remaining portion spans thicknesses of 3 to 11.2 m and 18.3 to 27.4 m. This particular layer, owing to its moderate permeability and productivity, can serve as the small-scale storage for groundwater extraction, suitable for dug wells, hand tube-wells, as well as shallow tube-wells.

Main Aquifer

In the studied region, the primary aquifer, which comprises fine-medium, medium, medium-coarse, and coarse sand, serves as a promising layer for the storage, and exploration of groundwater resources. The screens of deep tube wells are installed within this aguifer layer. The shaded contour maps in Fig. 5(c) depict the varying thickness of the primary aquifer. A substantial bed measuring between 42.7 and 67 m in thickness is distributed throughout the area, typically at depths ranging from 15 to 46 m. The presence of this substantial primary aquifer bed indicates that the region holds favorable conditions for the development of groundwater if other necessary requirements are met. The thickness characteristics of the aquitard, small-scale aquifer, and main aquifer are ranked based on their groundwater yield capacity, as illustrated in Fig. 5 and Table III.

3.1.5.2. Hydrostratigraphic Correlation

Groundwater potentiality estimation is made possible by sequence stratigraphy. Based on the dating of the various formations, as shown in the fence diagrams in Table IV, a generic hydrostratigraphic succession is provided for the studied region.

3.1.6. Rainfall and Groundwater

The prepared geospatial map for rainfall (Fig. 6(a)) classified the area into four categories ranging from 1462 mm to 1465 mm, 1465 mm to 1467 mm, 1467 mm to 1469 mm

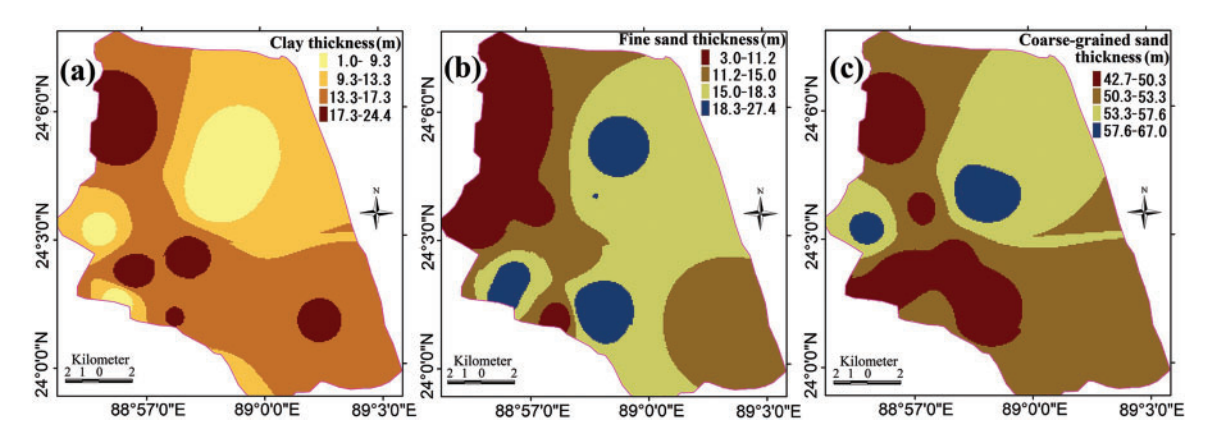


Fig. 5. Spatial variation of (a) Clay thickness, (b) Fine sand thickness, and (c) Coarse grained sand thickness.

and 1469 mm to 1473 mm extending from the north to the south. Here, higher importance was given to the higher values and vice-versa (Table III).

The assessment of the groundwater status in the area is based on the bimonthly water level data spanning from 2012 to 2020. Typically, two extreme positions are observed throughout the year: pre-monsoon and post-monsoon. The spatial distributions of the average annual water levels during these periods from 2012 to 2020 are presented in Figs. 6(b) and 6(c). In the pre-monsoon, the average depth to the water table is ranging from 3.12 to 3.86 m, while in the post-monsoon, these values vary from 6.97 to 8.36 m.

The groundwater-level records during the period of 2012-2020 for the area confirm that fluctuations occur within the upper clay-silt-very fine sandy layer. The specific yield value is determined as 0.1133, which is an average of 0.03, 0.08, and 0.23, as reported by Johnson in 1967, for clay, silt, and fine sand, respectively.

The spatial variation of average annual groundwater recharge map has been prepared and depicted in Fig. 6(d). The recharge varies from 0.4 m/yr to 0.59 m/yr.

3.1.7. Transmissivity

Equation (3) was applied to estimate the transmissivity of wells within the investigated area as shown in in Fig. 7(a). The transmissivity values vary from 2114 to 2591 m²/day, the average transmissivity being 2353 m²/day. The transmissivity of 2114–2347 m²/day prevails in most of the study area, while a few isolated pockets exhibit transmissivity values exceeding 2347 m²/day, primarily in the southeastern region. It's worth noting that the investigated area displays favorable characteristics for the development of groundwater, particularly in connection with its ability to transmit groundwater. The ratings for various transmissivity ranges have been estimated on the basis of their hydrogeological importance and are presented in Table III.

3.1.8. Hydraulic Conductivity

The hydraulic conductivity depicted in Fig. 7(b) was estimated through (4). The hydraulic conductivity within the area ranges from 28.2 m/day to 44.2 m/day. Most of the area has the hydraulic conductivity value of 28.2 m/day to 38.3 m/day. The higher values of hydraulic conductivity specify the more favorability for groundwater exploration. Higher ratings are set for higher values of this parameter and tabulated in Table III.

3.1.9. Specific Yield

Spatially depicted map for the specific yield computed through (5), is exhibited in Fig. 7(c). Various zones have been delineated based on its values from 18.9% to 26%. While there are isolated regions with specific yield values below 21.1% and above 23.5% scattered throughout the area, the maximum area lies within the specific yield range of 21.1% to 23.5%. This suggests the area's suitability for groundwater exploration. The ratings of the parameter are tabulated in Table III provided that higher ratings were set for higher parameter values.

3.2. Delineation of Groundwater Potential Zone Using

The themes were prepared using IDW interpolation method, and the features were categorized using Jenks optimization data clustering approach. The ratings of the features of the themes from their index values was calculated using Catastrophe theory.

The features (indicators) of all the themes (factors) except surface water bodies satisfy the butterfly model (Table II) where surface water body satisfies the swallowtail model. The average index of different themes was standardized using (8) and (9). From the standard quantities, the ratings of the features of the thematic layers were estimated using CT normalization methods (Table III). According to CT, the weights of thematic layers were determined by averaging the normalized values of each

TABLE IV: CORRELATION OF HYDROSTRATIGRAPHIC UNITS

Lithology	Depth (m)	Thickness (m)	Aquifer types
Clay with silt and sand	0	1–24	Aquitard
Fine sand with occasionally fine-medium sand	1-24	3–27	Small-scale aquifer
Fine-medium, medium-coarse and coarse sand	15–46	43–67	Main aquifer

layer. Table IV shows the results of utilizing CT to compute the ratings of the features and weights of themes.

The GWPI map generated with the aid of ArcGIS union tool using (7) is depicted in Fig. 8(a). The GWPI value in the area was found to range between 0.72 and 0.96. Three different groundwater potential zones with GWPI of 0.72-0.81, 0.81-0.87 and 0.87-0.96 were demarcated as moderately good, good and very good. The coverage of those zones in the study area was found 25.44%, 47.60%, and 26.96%, respectively. Groundwater potential zone marked as 'very good', likely to be of high yield capacity, was found in the study area's north, east and middle part near surface water bodies. A promising groundwater potential zone with GWPI values ranging from 0.81-0.87

was also distributed dominantly in the north to south through the eastern half, whereas the 'moderately good' groundwater potential zone was found in the western and southern sides.

3.3. Sensitivity Analysis

Tables V and VI show the mean change in GWPI when one or more layers are removed from the calculated GWPI in accordance with (10). Significant fluctuations in GWPI were observed when the rainfall having a mean variation index of 11.66% was excluded, whereas the lowest variation index of 3.88% was for land types. Furthermore, the GWPI seems to be moderately sensitive for hydraulic conductivity, coarse-grained sand thickness and recharge,

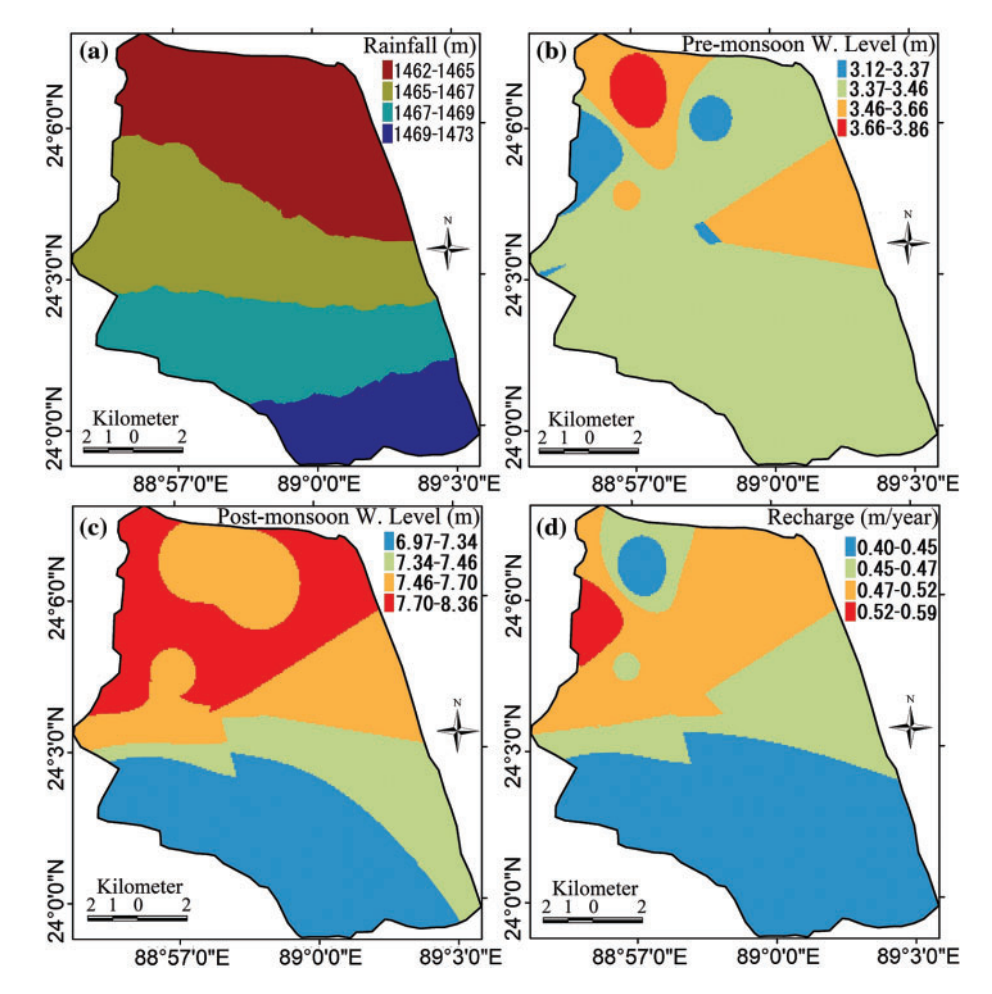


Fig. 6. Spatial distribution of (a) rainfall, (b) pre-monsoon water table, (c) post-monsoon water table, and (d) recharge.

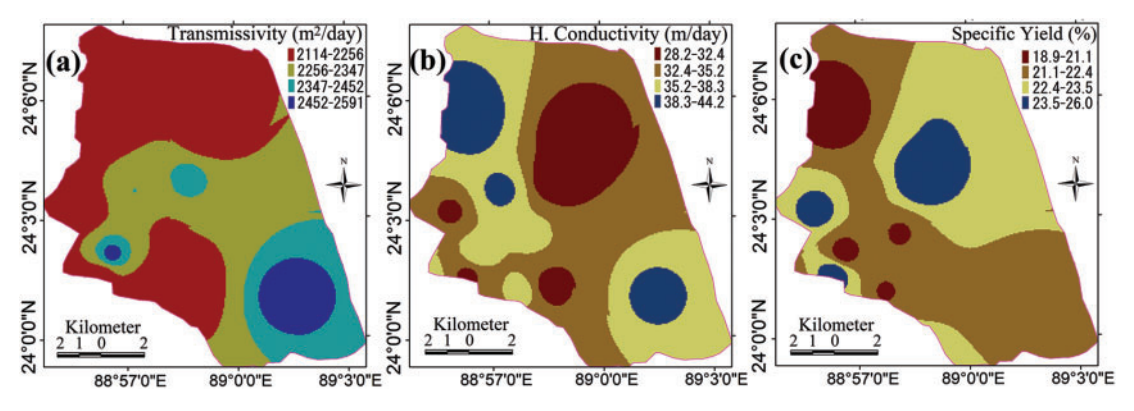


Fig. 7. Spatially distribution maps: (a) transmissivity, (b) hydraulic conductivity, and (c) specific yield.

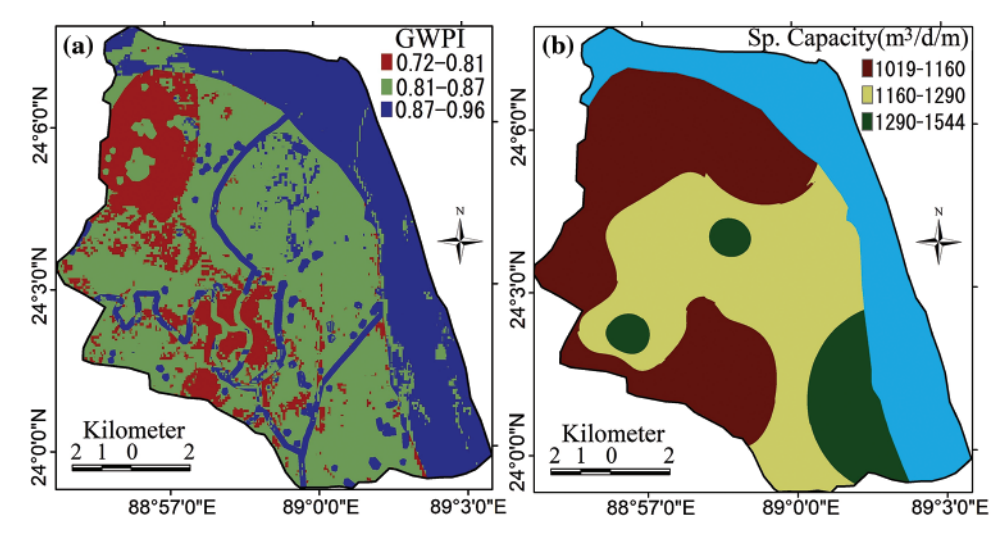


Fig. 8. Spatial maps: (a) groundwater potential index, (b) specific capacity.

TABLE V: STATISTICS OF THE ONE-MAP REMOVAL SENSITIVITY Analysis of Groundwater Potential

Parameter		Variation index (%)					
removed	Mean	Min	Max	SD			
RF	11.66	0.00	13.94	2.01			
T	11.17	9.54	13.42	0.67			
SY	11.15	9.73	13.38	0.66			
C	10.75	4.51	17.81	3.67			
HC	10.71	8.55	13.09	0.82			
CST	10.59	8.92	12.77	0.72			
R	9.69	0.00	13.15	2.58			
FST	8.25	5.08	11.56	1.33			
DD	6.45	0.00	9.68	2.23			
S	5.70	0.00	8.82	2.09			
SWB	4.03	0.00	9.20	3.82			
LT	3.88	0.00	8.65	1.40			

Note: RF-rainfall, T-transmissivity, SY-specific yield, C-clay thickness, HC-hydraulic conductivity, CST-coarse grained sand thickness, R-recharge, FST-Fine sand thickness, DD-drainage density, S-slope, SWB-surface water body and LT-Land Type.

as their mean variation index is 10.71%, 10.59% and 9.69%, respectively.

3.4. Validation

In this investigation, the validity of the GWPI model has been evaluated with the specific capacity estimated from available pumping test results (Fig. 8(b)). High specific capacity reflects high yield, and low specific capacity indicates low yield. Fig. 8(a) and Fig. 8(b) show that the area with lower specific capacity reflects the lower GWPI and vice-versa with a little discrepancy due to low data points.

4. Conclusions

Groundwater potential map for the area studied is derived by integrating hydro-geologically significant parameters using catastrophe theory. The region was categorized into moderately good, good and very good encompassing 25.44%, 47.60% and 26.96% area respectively. The classified groundwater potentials verified using

TABLE VI: SENSITIVITY ANALYSIS BASED ON ONE OR MULTIPLE THEME REMOVAL

Parameter	Variation index (%)					
	Mean	Min	Max	SD		
RF, T, SY, C, HC, CST, R, FST, DD, S, SWB	3.88	0.00	8.65	1.40		
RF, T, SY, C, HC, CST, R, FST, DD, S	7.91	0.00	17.84	4.23		
RF, T, SY, C, HC, CST, R, FST, DD	13.61	0.00	26.55	4.18		
RF, T, SY, C, HC, CST, R, FST	20.06	4.28	34.10	4.07		
RF, T, SY, C, HC, CST,R	28.31	14.80	44.08	3.92		
RF, T, SY, C, HC, CST	38.00	25.90	49.90	3.61		
RF, T, SY, C, HC	48.59	37.23	60.31	3.10		
RF, T, SY, C	59.30	49.57	70.68	2.72		
RF, T, SY	66.03	59.67	77.93	2.39		
RF, T	77.17	72.67	88.95	2.12		
RF	88.34	86.06	100.00	2.01		

specific capacity data estimated from available pumping test records shows a minimal discrepancy. The outcomes of the present study can guide the future groundwater exploration, planning and management.

Implementing the GIS-integrated catastrophe theorybased MCDA technique with the Jenks optimization data clustering method helps to avoid subjectivity in assessing the influence of different groundwater potential indicators, and thus, proves an unbiased estimate of groundwater potential. Thus, the use of CT for GWPI zoning made this study a potential pioneer for providing rapid, precise, and effective results. So, this methodology may easily be adopted for sustainable groundwater development in other similar areas. This research underscores the importance of employing evenly distributed observatory well data in order to validate the groundwater potential index in upcoming studies.

FUNDING

This research received funding from the Ministry of Science and Technology, Bangladesh.

CONFLICT OF INTEREST

The corresponding author declares no conflict of interest on behalf of all authors.

REFERENCES

- WEF (World Economic Forum). The Global Risks Report. Geneva, [1] Switzerland: World Economic Forum; 2016. http://www3.weforum. org/docs/GRR/WEF_GRR16.pdf.
- WWAP (World Water Assessment Programme). United Nations world water development report 3. Water in a Changing, 2009.
- Siebert S, Burke J, Faures JM, Frenken K, Hoogeveen J, Doll P, et al. Groundwater use for irrigation—A global inventory. Hydrol Earth Syst Sci. 2010;14:1863-80. doi: 10.5194/hess-14-1863-2010.
- Hasan MA, Ahmed KM, Sracek O, Bhattacharya P, Brömssen MV. Broms S. et al. Arsenic in shallow groundwater of Bangladesh: investigations from three different physiographic settings. Hydrogeol J. 2007;15(8):1507-22.
- Shahid S, Hazarika MK. Groundwater drought in the northwestern districts of Bangladesh. J Water Resour Manage. 2010;24: 1989–2006.
- MPO. National Water Plan Project-National Water Plan, vol. I. Dhaka: Master Plan Organization; 1991, pp. 109.
- WARPO (Water Resources Planning Organization of Bangladesh). National Water Management Plan of Bangladesh, Final Report. Bangladesh: Water Resources Planning Organization; 2001.
- BBS. Population census of Bangladesh: Bangladesh bureau of statistics, statistic division, ministry of planning, Government of the people's republic of Bangladesh; 2001.
- Momin MA. Impact of farakka barrage over the south-western region of Bangladesh. The International Conference. Dhaka. December 12, 2003. (Mimeographed).
- Haque MN, Keramat M, Shahid S. Spatial assessment of aquifer properties in a soft rock area of greater Kushtia district of Bangladesh. J Appl Hydrol. 2011;XXIV(1&2):9–18.
- [11] Haque MN, Keramat M, Shahid S. Groundwater resource evaluation in the western part of Kushtia district of Bangladesh using vertical electrical sounding technique. ISH J Hydraul Eng. 2015;21(1):97–110. doi: 10.1080/09715010.2014.981679
- [12] Haque MN, Shahid S, Keramat M, Mohsenipour M. GIS integration of hydrogeological and geoelectrical data for groundwater potential modeling in the western part of greater kushtia district of Bangladesh. Water Resour. 2016;43(2):283-91.
- [13] Shahinuzzaman M, Mostafa S, Uddin KMN, Islam MK, Alibuddin M, Haque MN. Hydrostratigraphy and its relation to groundwater potentiality of an area of the ganges river delta in Bangladesh. World J Eng Technol. 2016;4:10-20.
- [14] Das S, Pardeshi SD. Integration of different influencing factors in GIS to delineate groundwater potential areas using IF and FR techniques: a study of Pravara Basin, Maharashtra, India. Appl Water Sci. 2018;8:197. doi: 10.1007/s13201-018-0848-x.
- [15] Arulbalaji P, Padmalal D, Sreelash K. GIS and AHP techniques based delineation of groundwater potential zones: a case study from southern western Ghats, India. Sci Rep. 2019;9:2082. doi: 10.1038/s41598-019-38567-x.
- [16] Yang F, Shao D, Xiao C, Tan X. Assessment of urban water security based on catastrophe theory. Water Sci Technol. 2012;66:487-93.
- [17] Karanth KR. Hydrogeology. New Delhi: Tata McGraw-Hill Publishing Co. Ltd; 1989, pp. 458.
- [18] Shahid S, Nath SK, Roy J. Groundwater potential modeling in a soft rock area using GIS. Int J Remote Sens. 2000;21(9):1919-24.
- Shopan AA, Islam AKMS, Dey NC, Bala SK. Estimation of the changes of wetlands in the northwest region of Bangladesh using Landsat images. 4th International Conference on Water and Flood Management, Dhaka, Bangladesh, 2013.
- [20] Lasm T, Youan T, Baka D, Lasme Z, Oga MS, Jourda P, et al. Improvement of aquifer transmissivity assessment in crystalline and metamorphic fractured rocks in Bondoukou area. North-Eastern Côte d'Ivoire. Am J Sci Ind Res. 2012;3(5):315-30.
- [21] Morris DA, Johnson AI. Summary of Hydrologic and Physical Properties of Rock and Soil Materials, as Analyzed by the Hydrologic Laboratory of the U.S. Geological Survey, 1948-1960. USGS Water Supply Paper: 1839-D. Washington, DC: US Geological Survey; 1967, pp. 42.
- Johnson AI. Specific yield-Compilation of specific yields for various materials. U.S. geological survey water-supply paper, 1662-A.

- [23] Raleph RC. Basic Ground-Water Hydrology. U.S. Geological Survey Water-Supply Paper-2220. Washington, DC: U.S. Geological Survey; 1984, pp. 86.
- [24] Tritscher P, Read WW, Broadbrodge P. Specific yield for twodimensional flow. Water Resour Res. 2000;36:383-8.
- [25] Ghorbani MA, Khatibi R, Sivakumar B, Cobb L. Study of discontinuities in hydrological data using catastrophe theory. Hydrol Sci J. 2010;55:1137–51.
- [26] Kam JK. Are chaos and catastrophe theories relevant to environmental sciences. J Environ Sci. 1992;4:39-42.
- [27] Hui Q. Niche, Factor Interaction and Business Evolution—The Enterprise Niche Research of the Growth Business. Hangzhou: Zhejiang University Press; 2008.
- Ahmed K, Shahid S, Harun SB, Ismail T, Nawaz N, Shamsudin S. Assessment of groundwater potential zones in an arid region based on catastrophe theory. Earth Sci Inform. 2015;8(3):539-49. doi: 10.1007/s12145-014-0173-3.
- [29] Wang XJ, Zhang JY, Shahid S, Xia XH, He RM, Shang MT. Catastrophe theory to assess water security and adaptation strategy in the context of environmental change. Mitig Adapt Strateg Glob Chang. 2014;19(4):463-77.
- [30] Li P, Hui Q, Wu J -H. Groundwater quality assessment based on improved quality index in Pengyang County, Ningxia, northeast China. E J Chem. 2010;7(1):209–16.
- [31] Wang W, Liu S, Zhang S, Chen J. Assessment of a model of pollution disaster in near-shore coastal waters based on catastrophe theory. Ecol Model. 2011;222:307-12.
- [32] Al-Abadi AM, Shahid S, Al-Ali AK. A GIS-based integration of catastrophe theory and analytical hierarchy process for mapping flood susceptibility: a case study of TeebArea, Southern Iraq. Environ Earth Sci. 2016;75(8):687:1-19. doi: 10.1007/s12665-016-5523-7.
- [33] Al-Abadi AM, Shahid S. A comparison between index of entropy and catastrophe theory methods for mapping groundwater potential in an arid region. Environ Monit Assess. 2015;187(9):576. doi: 10.1007/s10661-015-4801-2e.
- [34] Hammouri N, El-Naqa A, Barakat M. An integrated approach to groundwater exploration using remote sensing and geographic information system. J Water Resour Prot. 2012;4:717-24
- [35] Kumar S, Machiwal D, Parmar BS. A parsimonious approach to delineating groundwater potential zones using geospatial modeling and multicriteria decision analysis techniques under limited data availability condition. Eng Rep. 2019;1:e12073. doi: 10.1002/eng2.12073
- [36] Cheng CH, Liu YH, Lin Y. Evaluating a weapon system using catastrophe series based on fuzzy scales. Soft Computing in Intelligent Systems and Information Processing. Proceedings of the 1996 Asian Fuzzy Systems Symposium, pp. 212-7, Kenting, Taiwan: IEEE, 1996. doi: 10.1109/afss.1996.583593.